

## One-dimensional transverse-field Ising model in a complex longitudinal field from a real-space renormalization-group method at $T = 0$

K. Uzelac,\* R. Jullien, and P. Pfeuty

*Laboratoire de Physique des Solides,<sup>†</sup> Université de Paris-Sud,*

*Centre d'Orsay 91405 Orsay, France*

(Received 3 December 1979)

The ground state of the quantum one-dimensional transverse-field Ising model in a longitudinal field is studied using a real-space renormalization-group method. The longitudinal magnetization in the ground state is calculated. Considering a real longitudinal field, this study provides an indirect investigation of the equation of state of the equivalent classical two-dimensional Ising model. Considering then the case of a purely imaginary longitudinal field, a new critical behavior is found which corresponds to the Yang-Lee edge singularity of the classical equivalent. In this last case the details of calculations and results are given, published earlier in a letter form.

### I. INTRODUCTION

#### A. One-dimensional transverse-field Ising model

The purpose of this paper is to study the ground-state properties of the one-dimensional quantum Hamiltonian

$$\mathcal{H} = - \sum_i (JS_i^x S_{i+1}^x + \Gamma S_i^z + h S_i^x), \quad (1)$$

where

$$S^x = \begin{pmatrix} 0 & 1 \\ 1 & 0 \end{pmatrix}, \quad S^z = \begin{pmatrix} 1 & 0 \\ 0 & -1 \end{pmatrix}$$

are a set of Pauli matrices on each site  $i$  of an infinite chain. The interaction constant  $J$  and the transverse field  $\Gamma$  are real parameters, while the longitudinal field  $h$  will be considered either real or purely imaginary ( $h \rightarrow ih$ ). In this later case a short account of the results has been already published.<sup>1</sup> While Hamiltonian (1) has been exactly solved for  $h = 0$ ,<sup>2</sup> there is no exact solution available in the case  $h \neq 0$ .

For  $h = 0$ , exact results<sup>2</sup> show that the one-dimensional (1D) transverse-field Ising model (1D TFI) undergoes a second-order transition at  $T = 0$ , by increasing  $\Gamma$ . For  $\Gamma/J < (\Gamma/J)_c = 1$  the ground state is twice degenerate, and there exists a nonzero longitudinal magnetization  $M_x \langle 0|S_i^x|0 \rangle \neq 0$  ( $|0 \rangle$  denotes the ground state). For  $\Gamma/J > (\Gamma/J)_c = 1$ , the ground state is a singlet and there is no longitudinal magnetization. In a recent paper<sup>3</sup> a newly developed real-space renormalization-group method has been applied successfully to this model (with  $h = 0$ ). The location of the transition, the components of the magnetization, the spin-correlation functions, and the critical

exponents characterizing the transition have been calculated and checked against the exact results. The present study can be considered as an extension of this earlier work in the presence of an extra longitudinal field.

An important motivation of the present study comes from the correspondence which exists between the 1D TFI and the classical 2D Ising model at finite temperature. Suzuki<sup>4</sup> has shown that the ground-state energy of the quantum TFI in  $D$  dimensions is equivalent to the free energy of a classical Ising model in  $(D + 1)$  dimensions with an interaction going to zero in  $D$  dimensions and to infinity in the  $(D + 1)$ th. Thus, the transition in the ground state by increasing  $\Gamma$  at  $h = 0$  of Eq. (1) has exactly the same critical properties as the transition in temperature of the classical Ising model in 2D solved by Onsager. Then by introducing a longitudinal field in the 1D TFI (playing the role of an external field in the classical equivalent) one can, indirectly investigate the equation of state of the classical 2D Ising model, which is not known exactly. But, even more interesting is the case of a purely imaginary longitudinal field which provides an indirect study of the so-called "Yang-Lee edge singularity" in two dimensions.

#### B. Yang-Lee edge singularity

In 1952, Yang and Lee<sup>5,6</sup> have first shown that the theory of phase transition is closely connected with the study of the distribution of zeros of the partition function for a given system. The knowledge of this distribution determines completely the equation of state. They have proved that, under a class of general conditions, this distribution  $g(\theta)$  lies on the unit

circle  $z = e^{i\theta}$  in the complex plane  $z = \exp(-h/kT)$  (or "activity" plane). This theorem is, in particular, verified for ferromagnetic spin  $-\frac{1}{2}$  Ising systems in 1D and 2D, and  $g(\theta)$  has been analytically determined in the one-dimensional case.<sup>6</sup>

Below the critical temperature ( $T < T_c$ ) the zeros are distributed on the whole unit circle. Above the critical temperature ( $T > T_c$ ) a gap of width  $2\theta_g(T)$ , containing the positive real axis, is opened. The edges of this gap, which correspond to given purely imaginary values of the field  $h = \pm ih_g(T)$  are now known as the "Yang-Lee edge singularities." By crossing the circle, the real part of the magnetization  $M(h, T)$  jumps by a quantity proportional to  $g(\theta)$ , which vanishes at the edge. The absence of zeros on the positive real axis for  $T > T_c$  corresponds to the absence of spontaneous magnetization when  $h = 0$ .

A recent increasing interest has been provided to this original way of investigating the equation of states. Efforts were developed in the calculation of  $g(\theta)$  which is not generally a trivial problem in more than 1D.  $g(\theta)$  has been determined exactly only for some simple or limiting cases: the Ising model with infinite range interactions where mean-field theory is exact,<sup>7</sup> the Ising model on a Bethe lattice,<sup>8</sup> the spherical model,<sup>9</sup> and the hierarchical model.<sup>10</sup> Numerical investigations, based on series-expansion calculations, have been performed in 2D and 3D for Ising,<sup>11,12</sup> classical  $n$ -vector models,<sup>13</sup> and quantum Heisenberg model.<sup>13</sup> The properties of  $g(\theta)$  and the connection with thermodynamics has been the subject of many studies.<sup>8,14</sup> Fisher<sup>12</sup> recently emphasized that the edge  $h = ih_g(T)$  can be viewed as a new critical point and that the concept of scaling and renormalization group could be applied. Using a field-theoretical renormalization group, he pointed out some general properties of this transition. The upper critical dimensionality appears to be  $D = 6$  and his study is done in  $\epsilon$  expansion near  $D = 6$ . All the usual scaling laws are valid. The universality is even larger since the exponents do not depend on the number of spin components. Only one exponent is sufficient to deduce all the others. The exponent describing the critical behavior of the density of zeros near the edge is defined as

$$g(\theta) \sim \text{Re}M \sim [h - ih_g(T)]^\sigma \quad (2)$$

This exponent  $\sigma$  is different from the exponent  $1/\delta$  characterizing the transition in a real field.

In the present study we investigate the Yang-Lee edge singularity of the 2D Ising model *indirectly* by introducing a purely imaginary longitudinal field in the 1D quantum equivalent. The real part of the longitudinal magnetization calculated in the ground state of the 1D TFI for imaginary longitudinal field will reflect the properties of the function  $g(\theta)$  for the 2D Ising model

## II. RENORMALIZATION-GROUP METHOD

### A. Real longitudinal field

To investigate the ground-state properties of Eq. (1), we use a real-space renormalization-group procedure introduced recently to study quantum systems.<sup>15,16</sup> We will follow closely the same procedure as in the case  $h = 0$ ,<sup>3</sup> and we will share the same notations, except that here, the transverse field is noted  $\Gamma$ . The method is an iterative method in which, if we drop a constant, the Hamiltonian takes the same form [Eq. (1)] at each step. At step ( $n$ ) we deal with spins  $\bar{S}_j^{(n)}$  and constants  $J^{(n)}$ ,  $\Gamma^{(n)}$ , and  $h^{(n)}$ .

We divide the chain into adjacent blocks of  $n_s$  sites. The Hamiltonian is then the sum over the block index  $j$  of an intrablock Hamiltonian

$$H_j^{(n)} = -J^{(n)} \sum_{p=1}^{n_s-1} S_{j,p}^{x(n)} S_{j,p+1}^{x(n)} - h^{(n)} \sum_{p=1}^{n_s} S_{j,p}^{x(n)} - \Gamma^{(n)} \sum_{p=1}^{n_s} S_{j,p}^z \quad (3)$$

and of an interblock Hamiltonian

$$H_{j,j+1}^{(n)} = -J^{(n)} S_{j,n_s}^{x(n)} S_{j+1,1}^{x(n)} \quad (4)$$

First we solve  $H_j^{(n)}$  exactly in the space of dimensionality  $2^{n_s}$  generated by the basis vectors  $|\epsilon_1, \dots, \epsilon_p, \dots, \epsilon_{n_s}\rangle$ , where  $\epsilon_p$  takes the values of  $+1$  or  $-1$  corresponding to the eigenstates of  $S_{j,p}^{z(n)}$ . The approximation consists in retaining only the two lowest-energy states: the ground state and the first excited state that we call, respectively,  $|+\rangle^{(n+1)}$  and  $|-\rangle^{(n+1)}$ :

$$\begin{aligned} |+\rangle^{(n+1)} &= \sum \lambda_{\epsilon_1, \dots, \epsilon_p, \dots, \epsilon_{n_s}}^{+(n)} |\epsilon_1, \dots, \epsilon_p, \dots, \epsilon_{n_s}\rangle, \\ |-\rangle^{(n+1)} &= \sum \lambda_{\epsilon_1, \dots, \epsilon_p, \dots, \epsilon_{n_s}}^{-(n)} |\epsilon_1, \dots, \epsilon_p, \dots, \epsilon_{n_s}\rangle. \end{aligned} \quad (5)$$

The corresponding eigenvalues  $E_+^{(n+1)}$  and  $E_-^{(n+1)}$  as well as the coordinates  $\lambda_{\epsilon_1, \dots, \epsilon_p, \dots, \epsilon_{n_s}}^{\pm(n)}$  are evaluated by standard computer diagonalization at each step.

We then introduce a new set of spin operators  $S_j^{\alpha(n+1)}$  ( $\alpha = x, y, z$ ) attached to each block  $j$ , the eigenstates of  $S_j^z(n+1)$  being precisely  $|+\rangle^{(n+1)}$  and  $|-\rangle^{(n+1)}$ . Using these new block-spin operators,  $H_j^{(n)}$  can be rewritten as

$$\begin{aligned} H_j^{(n)} &= -\frac{1}{2} (E_-^{(n+1)} - E_+^{(n+1)}) S_j^{x(n+1)} \\ &\quad + \frac{1}{2} (E_+^{(n+1)} + E_-^{(n+1)}) I_j^{(n+1)}, \end{aligned} \quad (6)$$

where  $I_j^{(n+1)}$  is an identity matrix.

Taking the matrix elements of the old spin operators into the new block states we obtain spin-recursion rela-

tions which have the following form:

$$\begin{aligned} S_{j,p}^{x(n)} &= A_p^{xx} S_j^{x(n+1)} + A_p^{xz} S_j^{z(n+1)} + B_p^x I_j^{(n+1)} , \\ S_{j,p}^{z(n)} &= A_p^{zx} S_j^{x(n+1)} + A_p^{zz} S_j^{z(n+1)} + B_p^z I_j^{(n+1)} , \end{aligned} \quad (7)$$

where the coefficients  $A_p^{\alpha\beta}$  and  $B_p^\alpha$  are functions of the coordinates

$$\begin{aligned} A_p^{xx} &= \sum \lambda_{\epsilon_1, \dots, \epsilon_p, \dots, \epsilon_{n_s}}^+ \lambda_{\epsilon_1, \dots, -\epsilon_p, \dots, \epsilon_{n_s}}^- , \\ A_p^{xz} &= \frac{1}{2} \sum (\lambda_{\epsilon_1, \dots, \epsilon_p, \dots, \epsilon_{n_s}}^+ \lambda_{\epsilon_1, \dots, -\epsilon_p, \dots, \epsilon_{n_s}}^- - \lambda_{\epsilon_1, \dots, \epsilon_p, \dots, \epsilon_{n_s}}^- \lambda_{\epsilon_1, \dots, -\epsilon_p, \dots, \epsilon_{n_s}}^+) , \\ B_p^x &= \frac{1}{2} \sum (\lambda_{\epsilon_1, \dots, \epsilon_p, \dots, \epsilon_{n_s}}^+ \lambda_{\epsilon_1, \dots, -\epsilon_p, \dots, \epsilon_{n_s}}^- + \lambda_{\epsilon_1, \dots, \epsilon_p, \dots, \epsilon_{n_s}}^- \lambda_{\epsilon_1, \dots, -\epsilon_p, \dots, \epsilon_{n_s}}^+) , \\ A_p^{zx} &= \sum \epsilon_p \lambda_{\epsilon_1, \dots, \epsilon_p, \dots, \epsilon_{n_s}}^+ \lambda_{\epsilon_1, \dots, \epsilon_p, \dots, \epsilon_{n_s}}^- , \\ A_p^{zz} &= \frac{1}{2} \sum \epsilon_p (\lambda_{\epsilon_1, \dots, \epsilon_p, \dots, \epsilon_{n_s}}^+ \lambda_{\epsilon_1, \dots, \epsilon_p, \dots, \epsilon_{n_s}}^- - \lambda_{\epsilon_1, \dots, \epsilon_p, \dots, \epsilon_{n_s}}^- \lambda_{\epsilon_1, \dots, \epsilon_p, \dots, \epsilon_{n_s}}^+) , \\ B_p^z &= \frac{1}{2} \sum \epsilon_p (\lambda_{\epsilon_1, \dots, \epsilon_p, \dots, \epsilon_{n_s}}^+ \lambda_{\epsilon_1, \dots, \epsilon_p, \dots, \epsilon_{n_s}}^- + \lambda_{\epsilon_1, \dots, \epsilon_p, \dots, \epsilon_{n_s}}^- \lambda_{\epsilon_1, \dots, \epsilon_p, \dots, \epsilon_{n_s}}^+) . \end{aligned} \quad (8)$$

To rewrite the Hamiltonian in terms of the new spin operators, we insert the expressions for  $S_{j,1}^{x(n)}$  and  $S_{j,n_s}^{x(n)}$  into the expression (4) for the interblock interaction (note that  $A_{\uparrow}^{\alpha\beta} = A_{n_s}^{\alpha\beta}$  due to block symmetry). Doing so, we generate a new Hamiltonian which contains many more parameters than Eq. (1). In fact these parameters are not independent, and their number can be reduced by an adequate spin-rotation transformation

$$\begin{aligned} S_j^{x(n+1)} &= \frac{A_{\uparrow}^{xx}}{\Delta} S_j^{x(n+1)} + \frac{A_{\uparrow}^{xz}}{\Delta} S_j^{z(n+1)} , \\ S_j^{z(n+1)} &= -\frac{A_{\uparrow}^{xz}}{\Delta} S_j^{x(n+1)} + \frac{A_{\uparrow}^{zz}}{\Delta} S_j^{z(n+1)} , \\ \Delta &= [(A_{\uparrow}^{xx})^2 + (A_{\uparrow}^{xz})^2]^{1/2} . \end{aligned} \quad (9)$$

This transformation can be inverted, and reporting the expressions into  $H_j^{(n)}$  and  $H_{j,j+1}^{(n)}$  we get

$$\begin{aligned} H_j^{(n)} &= -\frac{A_{\uparrow}^{xz}}{2\Delta} (E_-^{(n+1)} - E_+^{(n+1)}) S_j^{x(n+1)} \\ &\quad - \frac{A_{\uparrow}^{xx}}{2\Delta} (E_-^{(n+1)} - E_+^{(n+1)}) S_j^{z(n+1)} \\ &\quad + \frac{1}{2} (E_-^{(n+1)} + E_+^{(n+1)}) I_j^{(n+1)} , \\ H_{j,j+1}^{(n)} &= -J^{(n)} (\Delta S_j^{x(n+1)} + B_{\uparrow}^x I_j^{(n+1)}) \\ &\quad \times (\Delta S_{j+1}^{x(n+1)} + B_{\uparrow}^x I_{j+1}^{(n+1)}) . \end{aligned} \quad (10)$$

The Hamiltonian at step  $(n+1)$  is obtained by adding these two contributions and by summing over  $j$ . If we drop a constant term (which contributes to the ground-state energy) the Hamiltonian takes exactly form (1) but with the new Ising axis  $X$  (instead of  $x$ ) with new constants  $J^{(n+1)}$ ,  $\Gamma^{(n+1)}$ , and  $h^{(n+1)}$  given

by

$$\begin{aligned} J^{(n+1)} &= \Delta^2 J^{(n)} , \\ \Gamma^{(n+1)} &= (A_{\uparrow}^{xx}/2\Delta) (E_-^{(n+1)} - E_+^{(n+1)}) , \\ h^{(n+1)} &= (A_{\uparrow}^{xz}/2\Delta) (E_-^{(n+1)} - E_+^{(n+1)}) + 2J^{(n)} \Delta B_{\uparrow}^x . \end{aligned} \quad (11)$$

these expressions define a renormalization-group transformation. They can be integrated by machine up to a fixed-point Hamiltonian. In fact there are only two dimensionless parameters  $(h/\Gamma)^{(n)}$  and  $(\Gamma/J)^{(n)}$ , the recursion relations of which can be directly obtained from Eq. (11). The results for the fixed point depend only on the initial values of  $\Gamma/J$  and  $h/\Gamma$ . They will be presented and discussed in the following section.

The constant which has been dropped in the mapping can be kept at each step to construct the ground-state energy per site

$$\frac{E}{N} = \lim_{n \rightarrow \infty} \sum_n \left[ \frac{1}{2} (E_+^{(n+1)} + E_-^{(n+1)}) - J^{(n)} (B_{\uparrow}^x)^2 \right] / n_s^n . \quad (12)$$

Also, the magnetization components  $\langle S_i^x \rangle$  and  $\langle S_i^z \rangle$  in the ground state can be evaluated through the spin-recursion relations for the central spin of the blocks, in order to avoid edge effects,

$$\begin{aligned} S_{j,\rho_0}^{x(n)} &= \frac{A_{\rho_0}^{xx} A_{\uparrow}^{xx} + A_{\rho_0}^{xz} A_{\uparrow}^{xz}}{\Delta} S_j^{x(n+1)} \\ &\quad + \frac{-A_{\rho_0}^{xx} A_{\uparrow}^{xz} + A_{\rho_0}^{xz} A_{\uparrow}^{xx}}{\Delta} S_j^{z(n+1)} + B_{\rho_0}^x I_j^{(n+1)} , \\ S_{j,\rho_0}^{z(n)} &= \frac{A_{\rho_0}^{zx} A_{\uparrow}^{xx} + A_{\rho_0}^{zz} A_{\uparrow}^{xz}}{\Delta} S_j^{x(n+1)} \\ &\quad + \frac{-A_{\rho_0}^{zx} A_{\uparrow}^{xz} + A_{\rho_0}^{zz} A_{\uparrow}^{zx}}{\Delta} S_j^{z(n+1)} + B_{\rho_0}^z I_j^{(n+1)} , \end{aligned} \quad (13)$$

where  $p_0 = \frac{1}{2}n_s$  if  $n_s$  is even,  $\frac{1}{2}(n_s + 1)$  if  $n_s$  is odd. These recursion relations can be integrated up to the fixed point to give  $\langle S_i^{x(0)} \rangle$  and  $\langle S_i^{z(0)} \rangle$  as a function of  $\langle S_j^{x(n)} \rangle$  and  $\langle S_j^{z(n)} \rangle$  in the fixed point which are known. They are either 1 or 0 depending on the fixed point (see the results) and consequently,  $\langle S_i^{x(0)} \rangle$  and  $\langle S_i^{z(0)} \rangle$  can be evaluated through the iterative procedure.

### B. Complex longitudinal field

All the preceding calculations can be extended to the case of a complex field  $h = h' + ih''$ . Here the first difficulty arises from the non-Hermiticity of the Hamiltonian. The same problem has been encountered when applying a similar method to the Reggeon field theory.<sup>17</sup> Like there, one takes the advantage that the matrix representing the block Hamiltonian remains symmetric. Thus, the right eigenvectors have the same coordinates as the left eigenvectors (and they are not complex conjugate as in the Hermitian case). Also, the different eigenvectors are orthogonal in the sense of the regular product

$$\sum_k \lambda_k^i \lambda_k^j = 0 \text{ if } i \neq j. \quad (14)$$

So, it is convenient to normalize each eigenvector  $i$  by dividing the coordinates by the square root of the norm

$$N_i = \sum_k (\lambda_k^i)^2. \quad (15)$$

Note that this norm is generally complex. This was already the case in Ref. 16.

Another problem is the choice of the two levels we retain, since now, their energies are generally complex. By analytic continuation from the real case where  $h' = 0$ , we choose the two levels which have the lowest real parts. Then all the following calculations remain strictly the same. Note that also the spin-rotation formulas remain unchanged since the

simple product preserves the commutation rules.

In the general cases, where  $h = h' + ih''$ , all the parameters become generally complex through the recursion scheme. Two interesting limiting cases are  $h'' = 0$  where all the parameters remain real and  $h' = 0$ , where  $\Gamma$  and  $J$  remain real, while  $h = ih''$  remains purely imaginary.

## III. RESULTS AND DISCUSSION

### A. Real longitudinal field

The procedure described in the preceding section allows us to determine the renormalization-group trajectories in the parameter space. Let us choose here the two independent parameters  $\Gamma/J$  and  $h/\Gamma$ ; in the 2D classical analog they correspond, respectively, to  $T/J$  and  $h/T$ .

#### 1. Fixed points

When we start with  $h = 0$ , we end up either to the stable fixed point  $\Gamma/J = 0$ ,  $h/\Gamma = 0$  or to the other stable fixed point  $\Gamma/J = \infty$ ,  $h/\Gamma = 0$ , depending on the initial value of  $\Gamma/J$ . In presence of a finite  $h \neq 0$ , we always end up to the stable fixed point  $h/\Gamma = \infty$  whatever the initial value of  $\Gamma/J$  is. In other words, the longitudinal field is always relevant. These three trivial stable fixed points:  $(\Gamma/J = h/\Gamma = 0)$ ,  $(\Gamma/J = \infty, h/\Gamma = 0)$ , and  $(h/\Gamma = \infty)$  correspond, respectively, to an Ising chain without field, a set of independent spins in an applied  $z$  field, and a set of independent spins in an applied  $x$  field.

The only nontrivial fixed point is thus the unstable fixed point,  $h = 0$ ,  $\Gamma/J = (\Gamma/J)_c$  already studied in Ref. 3. This point becomes now twice unstable in the presence of a longitudinal field. The values of  $(\Gamma/J)_c$  already obtained for different block sizes<sup>3</sup> are reported in Table I. They asymptotically converge towards the exact value  $(\Gamma/J)_c = 1$  when  $n_s$  increases.

TABLE I. Our results for the location of the transition, different exponents, and the period  $x$  of the oscillation of the real part of the magnetization for  $n_s = 2, 3, 4$ , and 5.

$n_s$	2	3	4	5	Exact
$(\Gamma/J)_c$	1.27675	1.15470	1.10568	1.07971	1
$\beta$	0.40	0.19	0.195	0.155	0.125
$\delta$	5.	10.2	10.0		15
$\sigma$	0.28	-0.30	-0.24	-0.29	
$\eta_c$	0.08	-1.0	-0.96		
$x$	2.2	1.7	1.0	3.1	

## 2. Magnetization

The calculation of the magnetization components is performed as explained in the preceding section by expressing  $\langle S_i^{x(0)} \rangle$  and  $\langle S_i^{z(0)} \rangle$  as functions of  $\langle S_j^{x(n)} \rangle$  and  $\langle S_j^{z(n)} \rangle$  in the fixed point. The fixed-point values of  $\langle S_j^{x(n)} \rangle$  and  $\langle S_j^{z(n)} \rangle$  are

$$\langle S_j^{x(n)} \rangle_{n \rightarrow \infty} = \begin{cases} \pm 1, & \\ 0, & \\ +1, & \end{cases} \quad \langle S_j^{z(n)} \rangle_{n \rightarrow \infty} = \begin{cases} 0 & \text{for } \Gamma/J = h = 0, \\ +1 & \text{for } \Gamma/J = \infty, h = 0, \\ 0 & \text{for } h/\Gamma = \infty. \end{cases} \quad (16)$$

The average  $M_x = \langle S_i^{x(0)} \rangle$  and  $M_z = \langle S_i^{z(0)} \rangle$  can then be evaluated. We give an example of the results for  $M_x$  in Fig. 1 where we have plotted  $M_x$  as a function of  $\Gamma/J$  for different  $h/J$  values for  $n_s = 3$ . As expected the transition observed for  $h = 0$  disappears when  $h \neq 0$ .

The critical exponents directly related to the magnetization are  $\beta$  and  $\delta$  defined as

$$M_x \sim \begin{cases} \{(\Gamma/J - (\Gamma/J)_c)\}^\beta & \text{for } h/\Gamma = 0, \\ (h/\Gamma)^{1/\delta} & \text{for } (\Gamma/J) = (\Gamma/J)_c. \end{cases} \quad (17)$$

The exponent  $\beta$  was already calculated in Ref. 3. We present the results together with the values of  $\delta$  in Table I, for different  $n_s$  values. When  $n_s$  increases  $\delta$  converges slowly, with oscillations (due to the odd or even numbers of sites in the block) to the exact value  $\delta = 15$ .

## 3. Equation of state

The results for the equation of state, obtained for  $n_s = 3$  are represented in Fig. 2. The reduced longitudinal field  $\bar{h} = (h/M_x^\delta)/(h/M_x^\delta)_{\Gamma=\Gamma_c}$  has been plotted as a function of the reduced transverse field  $\bar{\Gamma} = x/C_\Gamma^-$  where  $x = (\Gamma/\Gamma_c - 1)/M_x^{1/\beta}$  and  $C_\Gamma^- = \lim_{\Gamma \rightarrow \Gamma_c} (-x)$ . The accuracy of the determination of  $\beta$  and  $\delta$  (within the approximations of the method) was tested from the condition of validity of

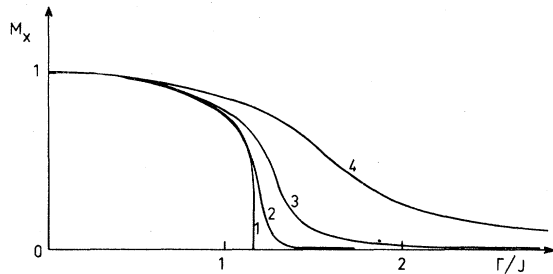


FIG. 1. Longitudinal magnetization  $M_x$  as a function of  $\Gamma/J$  for different real longitudinal fields, calculated for  $n_s = 3$ . The curves 1,2,3,4 correspond, respectively, to  $h/J = 0, 10^{-3}, 10^{-2}, 10^{-1}$ .

homogeneity properties, i.e., that the curves for  $\bar{h}/\Gamma$  between  $10^{-4}$  and  $10^{-8}$  coincide. The error for  $\delta$  is similar to that for the other exponents, of order 10%.

On Fig. 2, our results are compared with the equation of state for the 2D classical Ising model previously obtained by Gaunt and Domb<sup>18</sup> by series expansion calculation. The difference between our results and their results can be attributed to the different approximations used in the two cases. However, the slope of the two curves in the large field region are quite the same, because despite the errors of the method, our exponent  $\gamma$  is near the exact value.

An alternative (but not independent) more quantitative way to compare with series expansion results is to estimate the coefficients  $C_n^\pm$  as defined by Essam and Hunter.<sup>19</sup> In terms of these coefficients the equation of state of Fig. 2 can be represented by the following series:

$$x^{-\beta} = \sum_{n=1}^{\infty} \frac{C_{2n}^+}{(2n-1)!} \left( \frac{h/M_x^\delta \Gamma_c}{x^\Delta} \right)^{2n-1} \quad \text{for } x > 0, \\ (-x)^{-\beta} = \sum_{n=1}^{\infty} \frac{C_n^-}{(n-1)!} \left( \frac{h/M_x^\delta \Gamma_c}{(-x)^\Delta} \right)^{n-1} \quad \text{for } x < 0,$$

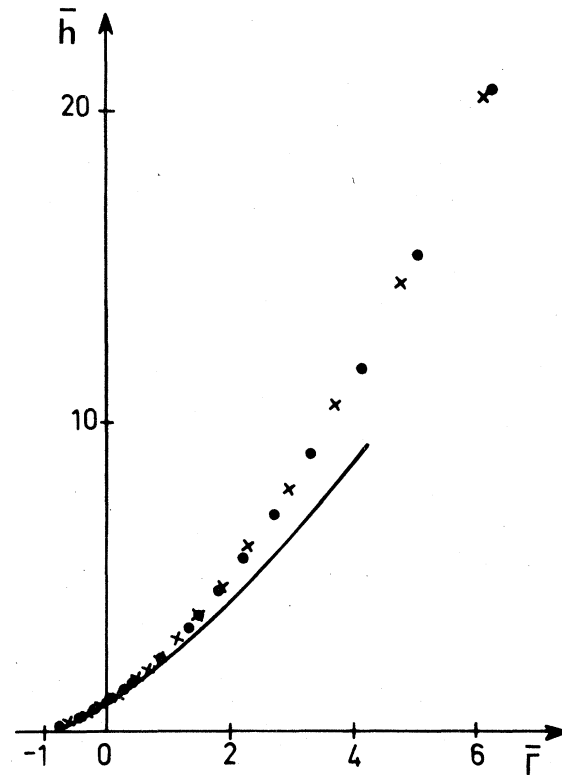


FIG. 2. Equation of states as a plot of  $\bar{h}$  as a function of  $\bar{\Gamma}$  ( $\bar{h}$  and  $\bar{\Gamma}$  are defined in text). Crosses and dots correspond, respectively, to  $h/\Gamma = 10^{-8}$  and  $10^{-4}$ . The results of Gaunt and Domb (Ref. 18) are represented by the continuous line.

TABLE II. Our estimates of the coefficient  $C_n^\pm$  (upper line) for  $n_s = 3$  compared with series-expansion results of Essam and Hunter (Ref. 19) for the square lattice in 2D (lower line).

	$C_2^+/2!$	$C_4^+/4!$	$C_6^+/6!$	$C_1^-/1!$	$C_2^-/2!$	$C_3^-/3!$
RG	0.480	-0.08	0.013	1.192	0.008	$\sim -6 \times 10^{-5}$
	$\pm 0.01$	$\pm 0.01$	$\pm 0.005$	$\pm 0.01$	$\pm 0.005$	
Series	0.4812	-0.1821	0.1761	1.222 41	0.012 84	-0.002 91
	$\pm 0.0007$	$\pm 0.0021$	$\pm 0.0027$	$\pm 0.000 46$	$\pm 0.000 06$	$\pm 0.000 03$

with  $x = (\Gamma/\Gamma_c - 1)/M_x^{1/\beta}$ . Taking our exponents  $\beta$ ,  $\delta$ , and  $\Delta$  we have estimated the first three coefficients above and below the transition by a least-squares fit of our results. Our estimates, obtained for  $n_s = 3$ , are reported in Table II and compared with the series expansion results for the 2D square lattice.<sup>19</sup> The agreement obtained is quite good for the first coefficient  $C_1^-$  and  $C_2^+$  while it is less good for the following. This is not surprising since it is known<sup>20</sup> that these coefficients are related with the  $n$ -points correlation functions which are certainly badly described for large  $n$  by our truncative scheme. A better agreement would have been certainly obtained for  $n_s = 5$ . However, our purpose here was not to obtain more precise results on the 2D Ising model than those previously obtained by other methods. We just wanted to show on an example that renormalization-group calculation on a quantum model is able to reproduce the equation of state of the classical equivalent<sup>21</sup> quite well and also to provide a test of our calculations in the case of a real longitudinal field before studying the case of a purely imaginary field.

### B. Purely imaginary longitudinal field

As mentioned in the introduction this case should be related to the classical 2D Ising model in an external imaginary field, where the critical behavior is known as the Yang-Lee edge singularity. In this section  $h$  will denote the imaginary part of the longitudinal field  $ih$ .

#### 1. Fixed points

The results of the study in the parameter space  $\Gamma/J, h/\Gamma$  are summarized in Fig. 3 for  $n_s = 3$ . We observe a completely different behavior than in the real field case. We obtain a phase diagram with a critical line  $(h/\Gamma)_g = f(\Gamma/J)$  separating two phases  $h/\Gamma > (h/\Gamma)_g$  (region I on Fig. 3) and  $h/\Gamma < (h/\Gamma)_g$  (region II on Fig. 3). The trajectories are represented on Fig. 3. If we start from region I, with  $h \neq 0$ , we

end up to the fixed point  $h/\Gamma = \infty$ ,  $\Gamma/J = 0$  (with  $h/J = \infty$ ) which corresponds to free spins in a purely imaginary field. If we start from region II we end up to the fixed point  $h/\Gamma = 0$ ,  $\Gamma/J = \infty$ , the same stable fixed point as that reached, with  $h = 0$ , by starting with  $\Gamma/J > (\Gamma/J)_c$ . There are now two nontrivial fixed points  $P_1$  and  $P_2$  with the critical line joining them.  $P_1(h/\Gamma = 0, \Gamma/J = (\Gamma/J)_c)$  is the zero-field unstable fixed point.  $P_2(h/\Gamma = 1, \Gamma/J = \infty)$  is a new fixed point unstable everywhere except when it is reached just on the critical line.

The two lowest-energy levels become rapidly complex conjugate when we start from phase I, leading to a purely imaginary gap for the whole chains, while they are real and nondegenerate when we start from phase II, leading to a real gap, as for  $h = 0$ ,  $\Gamma/J > (\Gamma/J)_c$ .

In the equivalence with the 2D classical system the critical line  $(h/\Gamma)_g = f(\Gamma/J)$  should be analyzed as the edge value  $h_g$  function of the temperature  $T$  above  $T_c$ . The critical curve  $(h/\Gamma)_g = f(\Gamma/J)$  goes to zero near  $P_1$  with a power law

$$(h/\Gamma)_g \sim [\Gamma/J - (\Gamma/J)_c]^\Delta, \quad (18)$$

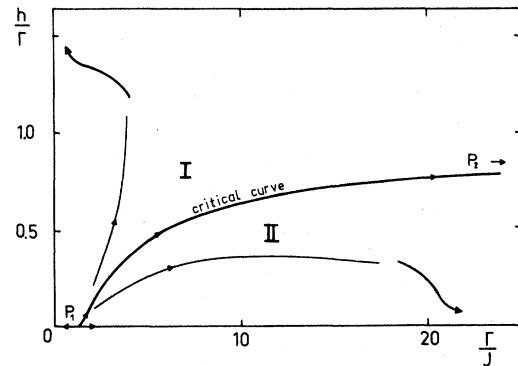


FIG. 3. Trajectories in the plane  $\Gamma/J, h/\Gamma$  where  $h$  is the imaginary part of the purely imaginary applied field plotted for  $n_s = 3$ . Ending of the trajectories are sketched by arrows.

where  $\Delta$  must be equal to  $\beta\delta$ .  $\Delta$  can be directly evaluated from the critical curve and then compared with  $\beta$  and  $\delta$ , calculated independently, and reported in Table I. We find that the scaling law  $\Delta = \beta\delta$  is well satisfied within the error bars. For example, for  $n_s = 3$  we find  $\Delta = 1.8 \pm 0.1$  while  $\beta\delta = 1.8 \pm 0.2$  from Table I (exact result is  $\Delta = 1.875$ ).

## 2. Magnetization and critical exponents

When crossing the critical line, there is a phase transition (when the gap becomes zero) which can be analyzed by looking at the magnetization. The longitudinal magnetization  $M_x$  is now a complex quantity. Figures 4 and 5 show  $\text{Re}M_x$  and  $\text{Im}M_x$  plotted as a function of  $h/\Gamma$  for different values of  $\Gamma/J$ , as they have been obtained by calculation for  $n_s = 3$ .  $\text{Re}M_x$  as a function of  $h/\Gamma$ , for a given  $\Gamma/J$ , corresponds to  $g(\theta)$  for a given temperature. As expected we find that  $\text{Re}M_x$  is zero, in region I [for  $h/\Gamma < (h/\Gamma)_g$ ]. Near  $(h/\Gamma)_g$ ,  $\text{Re}M_x$  has a divergency characterized by an exponent  $\sigma$  defined by

$$\text{Re}M_x \sim [h/\Gamma - (h/\Gamma)_g]^\sigma \quad (19)$$

We have checked the universality of  $\sigma$  by observing that it does not vary when crossing the critical line at different points. This is related to the fact that transitions on the critical line are all described by the unique fixed point  $P_2$ . Similarly, it does not depend on the direction of crossing. So, if we fix  $h/\Gamma$  and vary  $\Gamma/J$ , the corresponding critical exponent, that we call  $\beta_c$  in the analogy with the exponent  $\beta$  in the usual  $h = 0$  phase transition, is equal to  $\sigma$ . The exponent  $\sigma$  is negative and equal to  $-0.25 \pm 0.05$  for  $n_s = 3$ . The larger uncertainty is due to the oscillations in the curve which are still present near the transition. These oscillations will be discussed in the following. It is more easy to extract  $\sigma$  from the divergency of the imaginary part of  $M_x$ , which does not show any oscillations when approaching the critical line from  $h/\Gamma < (h/\Gamma)_g$ . The values of  $\sigma$  reported in Table I are obtained from  $\text{Im}M_x$ .

When comparing the three curves of Fig. 4, one can see the competition between the two fixed points  $P_1$  and  $P_2$  which becomes more pronounced as  $\Gamma/J$  diminishes. When  $\Gamma/J$  is close enough to  $(\Gamma/J)_c$  one can observe a crossover. As  $h/\Gamma$  diminishes,  $\text{Re}M_x$  first decreases with a positive exponent  $1/\delta$  and then increases with a negative exponent  $\sigma$ .  $1/\delta$  is the  $h = 0$  exponent characteristic of  $P_1$  while  $\sigma$  is the new exponent characteristic of  $P_2$ .

The second critical exponent  $\delta_c$ , which gives the variation of the magnetization by applying a small real field from the critical curve, comes out trivially. Namely, within a scaling approach, in the vicinity of the critical curve, real and imaginary perturbations in  $h$  will have the same scaling behavior, so that  $\sigma$  must

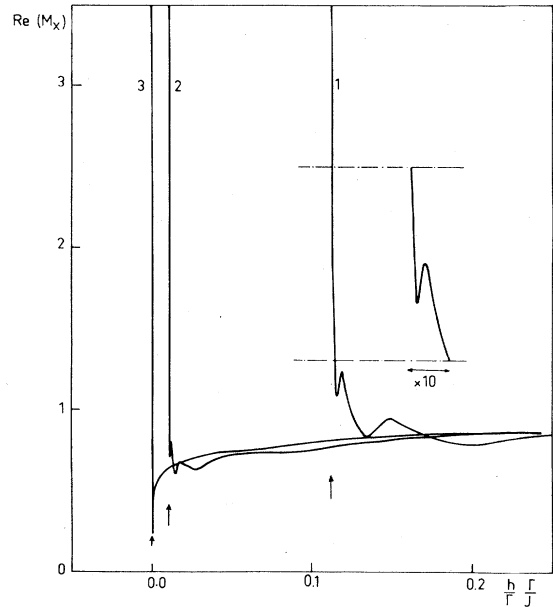


FIG. 4. Real part of the magnetization as a function of  $h/\Gamma$  for different  $\Gamma/J$  values, calculated for  $n_s = 3$ . Curves (1), (2), (3) correspond, respectively, to  $\Gamma/J = 1.7, 1.3, (\Gamma/J)_c + 10^{-3}$ . Vertical arrows show the location of the edge value  $(h/\Gamma)_g$  in each case. In the insert part of curve (1) is enlarged to show that oscillations are still present near the edge.

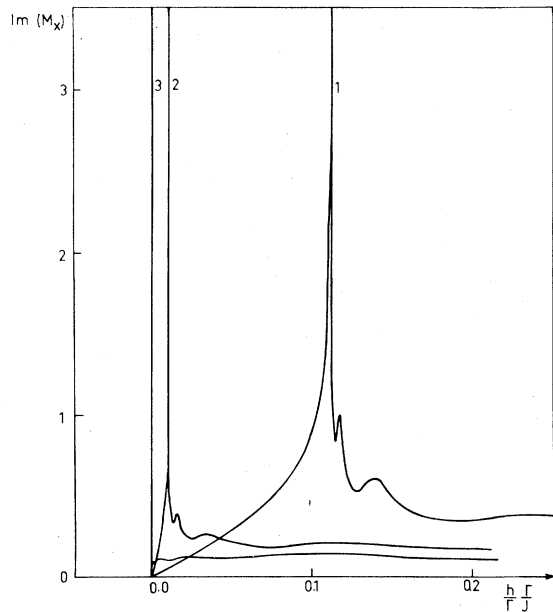


FIG. 5. Imaginary part of the magnetization as a function of  $h/\Gamma$  for different  $\Gamma/J$  values, calculated for  $n_s = 3$ . Curves (1), (2), (3) correspond to the same  $\Gamma/J$  values as in Fig. 4.

be equal to  $1/\delta_c$ . This is consistent with the fact that  $\text{Re}M_x$  and  $\text{Im}M_x$  should have the same singularities at the edge value  $(h/\Gamma)_g$ . This result leads to the exact value  $\Delta_c = \beta_c \delta_c = 1$ .

We have also extracted the exponent  $\eta_c$ , defined on the critical line, which describes the power-law behavior with distance of the  $x$ - $x$  spin-correlation function. This exponent has been evaluated from the renormalization of  $\text{Re}M_x$  for a trajectory along the critical line up to  $P_2$

$$\text{Re}M_x^{(n)} = \xi^{(n)} \text{Re}M_x^{(n+1)} \quad (20)$$

When one approaches  $P_2$ ,  $\xi^{(n)}$  tends to a constant value  $\xi$ . Then

$$\eta_c = 2 \ln \xi / \ln n_s \quad (21)$$

This exponent  $\eta_c$  is related with  $\sigma$  through the scaling law

$$\frac{1+z-2+\eta_c}{1+z+2-\eta_c} = \sigma \quad (22)$$

This formula is directly transposed from the scaling law relating  $\beta$  and  $\eta$  except that the dimensionality of the classical equivalent system ( $D=2$ ) has been replaced by  $1+z$  where  $z$  is the "dynamical" exponent describing the scaling of the energy for the 1D quantum model.  $z$  was defined precisely in Ref. 3. By calculating  $z$  at the edge, as already done without field in Ref. 3, it appears that the scaling law (22) is well satisfied within the error bars.

The results for the various exponents  $\sigma$ ,  $\eta_c$  are summarized in Table I for  $n_s = 2, 3, 4$ , and 5. For  $n_s = 2$ , the results are close to the mean-field results as already observed without longitudinal field: for  $\sigma$  we find a positive value  $\sigma = 0.28$  (the mean-field value is 0.5<sup>7</sup>). When  $n_s$  increases,  $\sigma$  becomes negative and shows some odd-even oscillations with  $n_s$ , as  $\beta$ . One can expect an asymptotic value for  $\sigma$  close to  $-0.27$ . This result for  $\sigma$  is definitively different than the exact 1D result for classical Ising systems  $= -0.5$ .<sup>6</sup>

However, our result is greater in absolute value than the estimations by high-temperature series for the susceptibility:  $\sigma = -0.12 \pm 0.05$ ,<sup>11</sup> and asymptotic high-temperature limit  $\sigma = -0.163 \pm 0.03$ .<sup>12</sup>

### 3. Oscillations of the magnetization

An advantage of the method presented here is that the whole curve  $\text{Re}M_x$  as the function of  $h/\Gamma$ , which corresponds to the distribution of zeros  $g(\theta)$  of the 2D Ising model, is obtained and not only its critical behavior near the edge characterized by the new exponent  $\sigma$ . A striking feature of the curves reported in Fig. 4 for  $n_s = 3$  is the oscillations in  $h$  which are still present near the edge (as shown by the enlargement of a part of one curve). It would be interesting

to know if these oscillations are due to the method or are characteristic of the real feature of the unknown function  $g(\theta)$ . These oscillations are present in the real part of the magnetization for all values of  $n_s$  that we have considered here. Figure 6 shows two examples of curve for  $n_s = 4$  and  $n_s = 5$ . These oscillations also exist in the imaginary part of  $M_x$  in region I while they are absent in region II. We have observed that the oscillations are periodic in  $\ln[h/\Gamma - (h/\Gamma)_g]$  so that formula (19) can be made more precise as

$$\text{Re}M_x \sim \left[ \frac{h}{\Gamma} - \left( \frac{h}{\Gamma} \right)_g \right]^\sigma \left( A + B \cos \left\{ \frac{2\pi}{x} \ln \left[ \frac{h}{\Gamma} - \left( \frac{h}{\Gamma} \right)_g \right] \right\} \right)$$

The period of the oscillations  $x$  depends on  $n_s$ . The results for  $x$  are reported in Table I. The fact that the oscillations are periodic in  $\ln[h/\Gamma - (h/\Gamma)_g]$  suggests an artifact of the method. Real-space renormalization-group methods produce in general errors each time the correlation length, which diverges as  $[h/\Gamma - (h/\Gamma)_g]^p$ , is equal to  $n_s^p$  (where  $p$  is an integer). This leads to oscillations periodic in  $\ln[h/\Gamma - (h/\Gamma)_g]$  with period equal to  $\ln \lambda_n = (1/\nu) \ln n_s$ .<sup>22</sup> Direct comparison with our results is difficult due to the fact that the way we calculate the magnetization creates another artifact: the odd-even oscillations in  $n_s$ . For this reason, we exclude the  $n_s = 4$  case which shows an anomalously small period and we compare the results for two odd values of  $n_s$ :  $n_s = 3$  and  $n_s = 5$ . The periods of the oscillations reported in Table I for these cases are not equal to  $\ln \lambda_n$ :  $\ln \lambda_n(n_s = 3) \sim 3$ ,  $\ln \lambda_n(n_s = 5) \sim 4.7$ , but

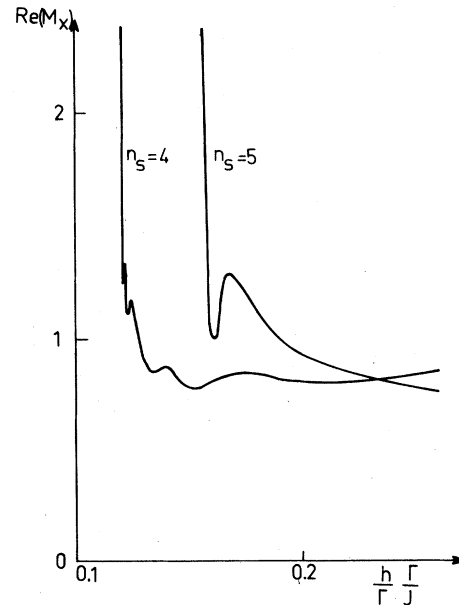


FIG. 6. Real part of the magnetization as a function of  $h/\Gamma$  for  $n_s = 4$ ,  $\Gamma/J = 1.65$  and for  $n_s = 5$ ,  $\Gamma/J = 1.7$ .

they seem to be proportional to  $\ln\lambda_n$ :  $x(5)/x(3) = 1.8$  while  $\ln\lambda_n(5)/\ln\lambda_n(3) \sim 1.6$ . To conclude we can say that an artifact of the method cannot be excluded.

#### IV. CONCLUSION

In conclusion, this study of the quantum 1D transverse-field Ising model in a longitudinal field was powerful to investigate the critical behavior of

the equivalent 2D classical Ising model in temperature. We have been able to evaluate the equation of state and we have given a calculation of the density of zeros of the partition function. We have found an edge exponent  $\sigma$  in reasonable agreement with previous estimations. Moreover, we have found a striking oscillatory behavior of the density of zeros which is probably due to the approximations of our renormalization-group method. It would be useful to extend the same study in higher dimensionalities as was already done without longitudinal field.<sup>23</sup>

<sup>1</sup>Permanent address: Institute of Physics of the University, Zagreb, Croatia, Yugoslavia.

<sup>2</sup>Laboratoire associé au CNRS.

<sup>3</sup>K. Uzelac, P. Pfeuty, and R. Jullien, *Phys. Rev. Lett.* **43**, 805 (1979).

<sup>4</sup>P. Pfeuty, *Ann. Phys. (N.Y.)* **57**, 79 (1970).

<sup>5</sup>R. Jullien, P. Pfeuty, J. N. Fields, and S. Doniach, *Phys. Rev. B* **18**, 3568 (1978).

<sup>6</sup>M. Suzuki, *Prog. Theor. Phys.* **56**, 1454 (1976).

<sup>7</sup>C. N. Yang and T. D. Lee, *Phys. Rev.* **87**, 404 (1952).

<sup>8</sup>T. D. Lee and C. N. Yang, *Phys. Rev.* **87**, 410 (1952).

<sup>9</sup>M. Suzuki, *Prog. Theor. Phys.* **38**, 1225 (1967).

<sup>10</sup>J. D. Bessis, J. M. Drouffe, and P. Moussa, *J. Phys. A* **9**, 2105 (1976).

<sup>11</sup>D. A. Kurtze and M. E. Fisher, *J. Stat. Phys.* **19**, 205 (1978).

<sup>12</sup>G. A. Baker, M. E. Fisher, and P. Moussa, *Phys. Rev. Lett.* **42**, 615 (1979).

<sup>13</sup>J. P. Kortman and R. B. Griffiths, *Phys. Rev. Lett.* **27**, 1439 (1971).

<sup>14</sup>M. E. Fisher, *Phys. Rev. Lett.* **40**, 1610 (1978).

<sup>15</sup>M. E. Fisher (unpublished).

<sup>16</sup>R. Abe, *Prog. Theor. Phys.* **38**, 72 (1967); G. A. Baker, *Phys. Rev. Lett.* **20**, 990 (1968); D. S. Gaunt and G. A. Baker, *Phys. Rev. B* **1**, 1184 (1970); G. A. Baker and J. Moussa, *J. Appl. Phys.* **49**, 1360 (1978); M. Barnsley, D. Bessis, and P. Moussa, *J. Math. Phys.* **20**, 535 (1979).

<sup>17</sup>S. D. Drell, M. Weinstein, and S. Yankielovicz, *Phys. Rev. D* **14**, 487 (1976).

<sup>18</sup>R. Jullien, J. N. Fields, and S. Doniach, *Phys. Rev. B* **16**, 4889 (1977).

<sup>19</sup>J. L. Cardy, *Nucl. Phys. B* **115**, 141 (1976).

<sup>20</sup>D. S. Gaunt and C. Domb, *J. Phys. C* **3**, 1442 (1970).

<sup>21</sup>J. W. Essam and D. L. Hunter, *J. Phys. C* **1**, 392 (1968).

<sup>22</sup>B. M. McCoy and T. T. Wu, *Phys. Rev. B* **18**, 4886 (1978).

<sup>23</sup>Let us mention that K. Subbarao, *Phys. Rev. Lett.* **37**, 1712 (1976), has obtained the equation of state for the 2D quantum Ising model (equivalent to the 3D classical Ising model) by using a quite different RG procedure from that used here.

<sup>24</sup>M. Nauenberg, *J. Phys. A* **8**, 925 (1975).

<sup>25</sup>K. A. Penson, R. Jullien, and P. Pfeuty, *Phys. Rev. B* **19**, 4653 (1979).